

Volumetric erosion of a structured electrical contact surface using X-Ray Computed Tomography.

J.W. McBride, University of Southampton, UK, jwm@soton.ac.uk

T.G. Bull, University of Southampton, UK.

K.J. Cross, TaiCaan Technologies Ltd, Southampton, UK. Kevin.Cross@taicaan.com

Abstract

The use of 3D optical scanning methods is well established for the evaluation of volumetric wear on electrical contact surfaces. A longstanding limitation of these methods has been the accuracy to which the underlying form of the surface prior to the wear process is determined. Electrical contact surfaces are never perfectly flat, in many applications the underlying surface is nominally spherical or a freeform surface. This paper introduces newly developed methods to enhance the capability of resolving volumetric wear on a surface with complex shape (form). These methods are applicable to a wide range of applications, but the focus here is on arcing electrical contacts. The paper investigates wear on a nominally spherical AgNi contact used in low voltage switching applications and compares this to the wear on a surface modified using electron beam process to create a highly structured surface; under the same switching conditions. The spherical contact is analysed using a new 3D optical metrology solution using a data fusion method, which combines both metrology data and surface photographic image data. The 3D optical scanning data is then compared with surface data from X-Ray computed tomography (X-CT) of the structured electrical contact surface.

1 Introduction

This paper focuses on wear related to arcing devices although the methods discussed are applicable to other electrical contact applications and to other types of surfaces. Many studies over the last 30 years have investigated mass transfer processes linked to arcing in switching contacts. **Figure 1** shows example results of such a study, [1]. It shows that the transfer between the anode and cathode surfaces in a 64 V DC resistive switching circuit related to the current level (0-16 A). With the transfer between the anode and cathode reversing above 3A, linked to the onset of a gaseous arc. The results in [1] showed one of the first applications of 3D surface data, with the data collected using a stylus profiling system. The onset of optical methods for the 3D surface profiling [2] generated a number of studies on the volumetric wear of electrical contacts [2-8]. Showing two key advantages over the stylus methods; Firstly, the contact surfaces do not need to be removed from the support to evaluate the surfaces; secondly the ability to differentiate between wear both above and below a set datum, as shown in **Figure 2**.

The detection of wear on a complex surface can be applied in many applications and in all cases, there are a number of fundamental issues;

1. The precision of the measurement system
2. The accuracy of the volume algorithms
3. The methods used to identify the underlying surface form, examples include; (a) Flat, (b) Spherical, (c) cylindrical, (d) toroidal, (e) free-form, (f) structured

surfaces no recess, and (g) structured surfaces with recesses.

1.1 Arc Wear Transport between Electrical contact surfaces

The wear process in electrical contacts with arcing is very complex, as reflected in the number of research publications in the field, [9]. The key issue is that the wear is a complex interaction of many variables, here separated into 5 categories, as shown in **Table 1**. Because of the complexity it is often difficult to determine underlying phenomena, with the results only relating to the specific conditions used. To reduce the complexity, control of the independent variables is used, [1]. For example, the data in **Figure.1**, is for a fixed DC voltage, with a resistive load, with a single material and constant opening velocity; thus controlling 2 of the variable categories. The remaining categories will have a significant influence on the resulting wear, it is therefore important to clearly define these. In this study, we investigate a controlled experimental condition with modern surface scanning instruments to provide information around the interaction of surfaces (anode and cathode).

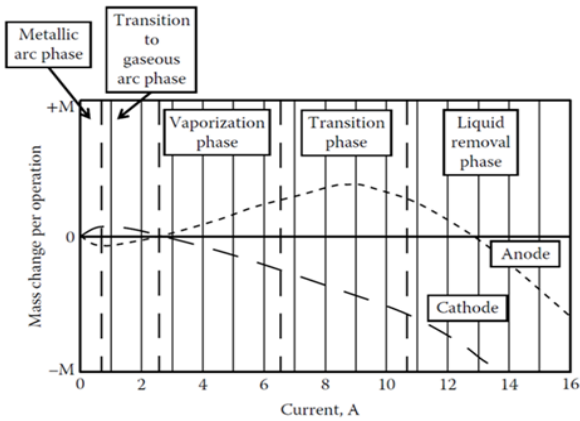


Fig.1 Mass Transfer, 60 VDC Break only, Ag MeO contacts, constant velocity (0.1m/sec) [1].

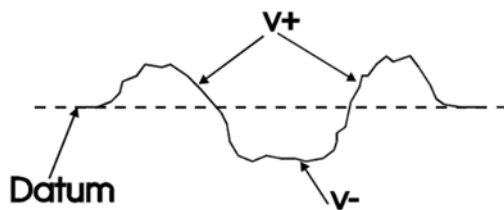


Fig. 2 Volume above and below a fixed datum surface.

1	Circuit conditions	Supply voltage V (AC DC), I, Load type.
2	Device design	Contact velocity, number of bounces on closure, interaction with magnetic fields, surrounding enclosure materials.
3	Experiment condition	Make only, Break Only, Point on Wave, Make and Break
4	Electrical contact material	Ag, Ag/Ni, Ag MO, etc
5	The environment	Temp, Pressure, humidity, vibration levels.

Table 1. Factors influencing the wear and erosion of electrical, contact switching surfaces.

2. Experimental Methods and Data Resolution

2.1 Test Fixture

A model relay mechanism is used, as shown in **Figure 3**, with two commercial contact rivets, Ag/Ni, (80/20). The lower contact is a fixed cathode; the moving contact has a maximum contact gap pre-set of 0.3mm. The moving contact is in the normally open condition and actuated by a standard (14V) relay coil. The circuit conditions used are, 14.8 V (DC), 10.2 A, resistive load, the contacts are switched for 3000 operations with both make a break cycles. Two surface types are used; in Experiment (1), a standard rivet contact; and in

Experiment (2) the same material as (1), modified to a predefined structured surface, shown **Figure 4**.

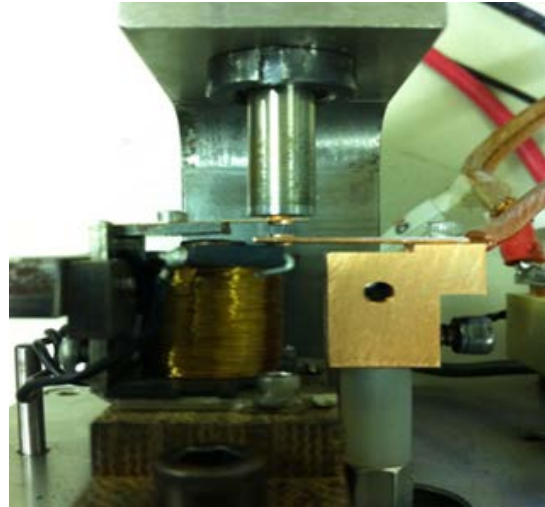


Fig. 3. The experimental test set up, with a fixed cathode and moving anode contact, actuated by the relay coil.



Fig. 4 Ag/Ni contact processed by electron beam processing, to create a highly structure surface.

2.2 The Structured Electrical Contact Surface

The structured electrical contact surface used in Experiment (2) is shown in **Figure 4**, it was modified using an electron beam processing method, [10]. When the electron beam comes into contact with the surface it melts and vaporises the material. Providing that the beam does not penetrate the surface, the vapour pressure of the molten material causes the material to be expelled from the hole formed. This material is deposited around the perimeter of the hole. A series of electro-magnetic coils are used to focus the electron beam and then deflect it around the material in a rapid and controlled manner, allowing this process to be carried out at many sites consecutively. In this study the resultant surface is the same material as the commercial

Ag/Ni rivet, (80/20) with the same overall dimensions. The surface exhibits a structure with a very high degree of surface roughness as shown in **Figure 4**.

2.3 Optical and X-Ray Surface Metrology Hardware and Software

The optical 3D surface metrology instruments used in this study is the TaiCaan Technologies XYRIS 2020. This is a calibrated metrology instrument. It is a new class of instrument (released in 2020), which combines an ability to measure surfaces with significant slope, with the ability to view the samples via microscope and scan over large areas. Two optical sensors have been used in this paper, the XYRIS 2020 L and H, where the L refers to a low gauge range sensor with high resolution (10 nm) and the H sensor is a high gauge range with a lower resolution of (25 nm).

X-Ray Computed Tomography (X-CT) has been used for many years in medical applications. Recent developments in metrology have seen increasing use of the method for precision metrology in engineering applications, [11-13]. The systems are not calibrated, and as such the optical data produced from the XYRIS 2020 H/L can be used to give an indication of the accuracy of the X-CT system. The system used here is a Nikon 225 kVp Nikon/Xtek HMX, used with the commercial software VGStudio Max 2.1 used to generate the surfaces. The data is 8-bit, and the size of scan (8mm x 5mm x 8mm), with as resolution, of $X=0.0048$, $Y=0.0048$, $Z=0.0048$ (mm). The point cloud data produced requires a further step in processing to detect the surface and to then render the surface. The render settings used a tool within VGStudio Max 2.1 to specify a sample of the background and a sample of the volume of interest, which then automatically, adjusted the histogram. The precision of the meshing was set to very precise with no simplification.

Both XYRIS and X-CT systems have commercial software tools, which enable the generation of the 3D data for processing. The data format used is a standard 3D point cloud format (STL) for the X-CT system. The XYRIS system generates both STL format data and a standard metrology format surface (2.5D) data (*.tai). The formats are imported @BEX [14], for analysis of the dimensional and volumetric data.

2.4 Defining the accuracy of the volumetric wear as a function of the metrology systems and software

There are a number of critical factors in defining the accuracy of volume measurements;

1. The accuracy of the measurement process. The system (XYRIS 2020 H) has a volume resolution of (X,Y,Z,) 100 nm, 100 nm, and 25 nm. If we use the

term VOXEL used in XCT to define volume resolutions, and assume Z to be the same as X,Y then the XYRIS Voxel size is 0.1 μm . The Voxel size of the X-CT system is correspondingly 4.8 μm , or approximately 50 x larger than the optical method. For both system the resolution does not directly relate to accuracy of the systems. The accuracy is a function of systematic and other errors. For the X-CT this is very complex and undefined. For the XYRIS 2020 H, the repeatability in X,Y of 150 nm and a noise floor in Z of 84 nm, for the L sensor the corresponding values are X,Y of 150 nm and a noise floor in Z of 24 nm. These combined to define the volumetric accuracy of the system used as (H sensor) 172 (cubic nm). Both the resolution and the accuracy are significantly higher when compared to the data in [1-7].

2. The X-CT system has a second stage of errors associated with the surface generation processes, which adds a further level of complexity to a system which has already poorly defined accuracy.

3. The accuracy of the software approach used to determine the volume. Some existing commercial software packages used to define volume have been shown to have errors of 9% when compared to reference data sets. Care must be used when selecting the appropriate methods. The software package used here is @BEX (TaiCaan Technologies) with a defined software error on a reference surface of <0.003%.

4. The accuracy of the form fitting methods used to remove the underlying form. The results of the volumetric wear are highly sensitive to selection of the area and the fitted surface. This is discussed in the results of experiment (1). The form fitting of a surface and the link to before and after studies leads to an introduction of the topic of data registration, [11], discussed briefly below.

2.5 The Characterisation of a Structured Electrical Contact Surface

Regular surfaces can be described by a number of parameters the most common of which are the two amplitude roughness parameters, R_a and R_q ; the former the arithmetic mean value of a rough surface and the latter the Root Mean Square or standard deviation of the surface. The 2D parameters are matched by the standard 3D amplitude parameters S_a and S_q . These values both R and S are taken relative to a nominal form fit and waviness filter (Gaussian). These parameters are crude descriptors proving no indication of the nature of the surface, as this requires both spatial and

amplitude information, along with some function describing the functionality of the surface, which in turn will be related to the application of the surface.

To allow the combination of both amplitude and spatial data a hybrid parameter is used we define as Sap. This areal parameter, (S type) and has been developed for the optimisation of electrode surfaces where the surface area is a key design parameter. A scale for texture ratio is used to define the increase in surface area caused by the texture. For an ideal smooth plane surface, the texture ratio (Sap) is 1.

$$\text{Texture Ratio} = \frac{3D \text{ Surface Area}}{\text{Projected Surface Area}}$$

The texture ratio parameter is similar to the Sdr parameter as defined by ISO25178 – Developed Interface Area Ratio – which describes how much the texture increases the surface area from a 2d plane but is less useful as it results in a 0 value for a plane surface as it is calculated by;

$$S_{dr} = \frac{3D \text{ Surface Area} - \text{Projected Surface Area}}{\text{Projected Surface Area}}$$

2.6 Data Registration to detect surface changes.

Data registration is a process where before and after (wear study) data is registered such that surfaces can be subtracted to determine the wear relative to the know datum. The registration problem is mathematically complex and a subject of major interest in a range of applications, [11]. We use surface that were not measured before testing, and in this case the underlying form is assumed to be a known geometric form, i.e. flat, spherical, etc. [1-7]. The natural contact rivets used are not high precision components and as such there will be errors in the underlying form evaluation as these are not perfectly spherical, as discussed below.

3. Results and Discussion

3.1 Experiment 1. Standard Electrical Contact, Ag/Ni 80/20, 3000 operations make and break.

Figure's 5 and 6 show the cathode and anode surface, measured using the XYRIS 2020H. It shows that the H sensor range allows the capture of both the base and the pip and crater wear. Figure 7 shows the application of data fusion with the anode surface height rendered with the photographic colours. This technique allows the user to define regions of wear which are not apparent in the 3D data. An example is the region surrounding the wear crater in Figure 6, which shows a darkened area.

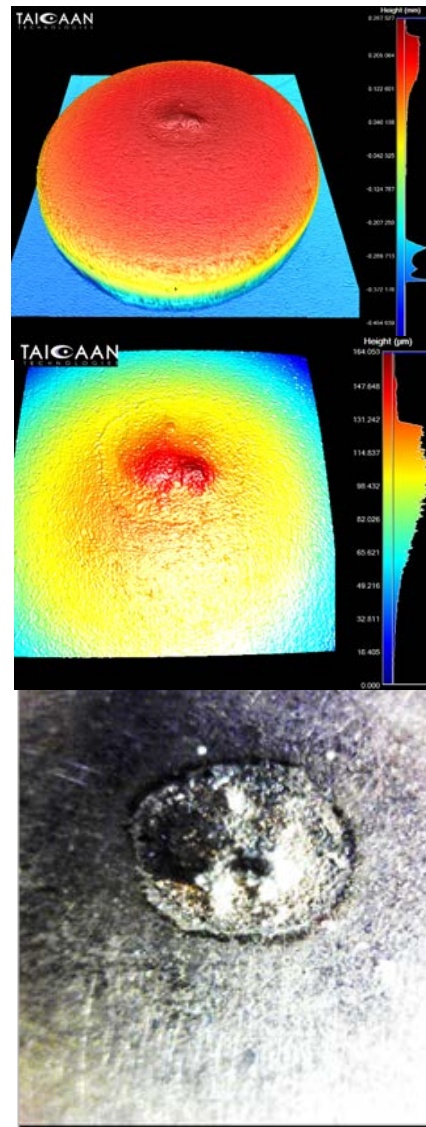


Fig. 5 Cathode; 14.8 V (DC), 10.2 A resistive load, 3000 switching operations with both make a break cycles. Ag/Ni. (80/20), (a) 2.6 mm x2.6 mm, (b) 1.5mm x 1.5mm, (c) microscope image.

	Exp. 1 (Cathode)	Exp.1 (Anode)	Exp. 2 (Anode)
Volume (Above)	2.86	0.271	0.582
Volume (Below)	-0.093	-3.701	-3.513
Volume Change	2.767	-3.43	-2.931

Table 2. Volumetric data Exp. 1 as shown in Fig's 5-8, and Exp. 2 in Fig. 9, all x10⁻³ mm³.

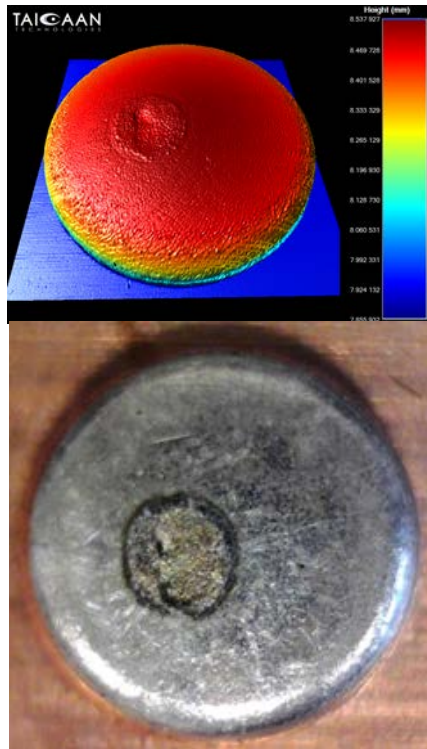


Fig.6 Anode Surface; 14.8 V (DC), 10.2 A resistive load, 3000 switching operations with both make a break cycles. Ag/Ni. (80/20); (a) 2.6 mm x 2.6 mm, (b) microscope image.

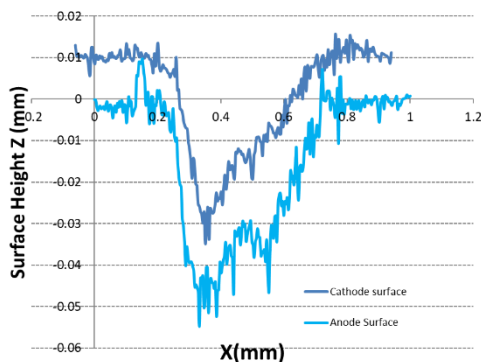


Fig.7 Cross section data through the pip and crater formation in Fig's 5 and 6, with the surfaces separated by 1 μ m.

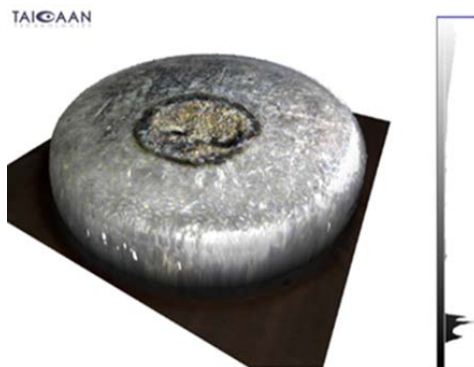


Fig.8 2D data superimposition. (a) Combining 2D data from Fig 5 and Fig 6.

The analysis of the volume information in **Figure's. 5 & 6**, follows an established 3 step methodology.

- Step 1; apply a 2D 80 μ m gaussian filter to the measured data, showing the changes in surface roughness only. This allows the identification of the wear region.
- Step 2; remove the region and fit a sphere to the residual surface. Replace the wear region to the levelled residual data.
- Step 3; remove the datum surface, using the region identified in Step 1 and determine the volume above and below the datum.

The results of the volumetric erosion are shown in **Table 2**. As evidenced by the difference in the net cathode gain and the net anode loss, some material is lost to the environment. This observation is further confirmed in **Fig.7**, which shows a cross section of the wear region with the cathode surface inverted onto the anode surface. It shows a close match, but it is clear that the material gained on the cathode is less than the material lost from the anode. This suggests that material is lost to the environment as shown by the volume differences. **Table 3** shows the roughness parameters of the undamaged surface, and the evaluation of the hybrid Sap parameter. To show the sensitivity to the form fitting process, the position of the datum surface can be adjusted in software, to show a shift of 1 μ m, reduces the negative wear volume by 15%. This emphasizes the sensitivity of the datum surface definition to any analytical evaluation of the volumetric data. To overcome this limitation would require a data registration process, [11].

	XYRIS H (Optical) Experiment 1	XYRIS L (Optical) Experiment 2	Nikon (X-CT) Experiment 2
Ra	1.545 μ m	52.015 μ m	45.781 μ m
Rq	1.96 μ m	58.95 μ m	53.187 μ m
Rz	13.91 μ m	237.93 μ m	225.31 μ m
X 4 peaks)	N/A	0.635 mm	0.639 mm
S a/p	1.094 (0.5 mm)	2.41* (1 mm)	1.924 (1 mm)

Table 3 Metrology data comparison, Experiment 1 and 2.* the optical data requires smoothing using Median filters

3.2 Structured cathode surface with regular anode surface, Ag/Ni 80/20, 3000 operations make and break

The electron beam modified electrical contact surface, (cathode or fixed contact) is shown in **Figure 9**. It shows a highly structured surface measured with the X-

CT system, with a cross section, showing recessed surface, i.e. where there is an overhang and where top down optical sensing would not be able to show the corresponding hidden surface. The data shows the height data from the X-CT measurement and associated surface rendering process as described above. The features in the surface as shown in the cross section correspond to holes in the surface with a typical depth of 0.16 mm. The resultant surface shows a number of peaks and a wear area is apparent in the microscope image, in **Figure 4** (darkened area), but not apparent in the 3D X-CT data.

The corresponding data from the optical system (XYRIS 2020 L) is shown in **Figure 10**, in this case for both the cathode surface and the anode surface. The optical measurement of the cathode surface is with higher resolution when compared to the X-CT data, but because of the line of sight issue, is unable to show the recessed surfaces.

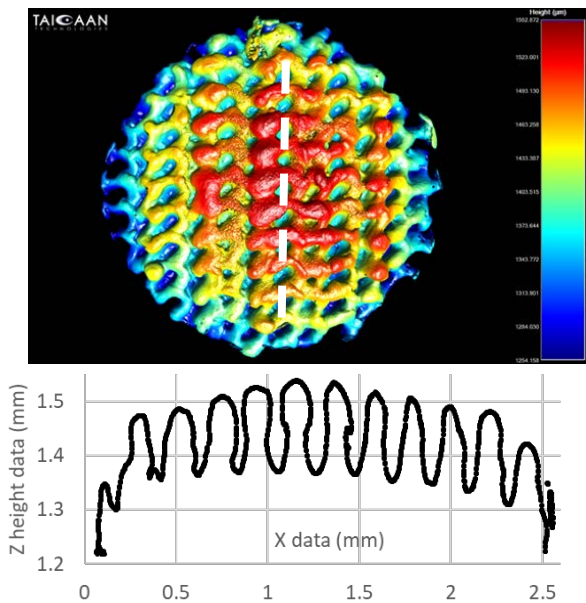


Fig 9. Structured cathode surface, using X-CT and surface generation, with cross section, through the white line.

3.3 Characterisation of the Surfaces.

The roughness values for the surfaces are shown in **Table 3**. It is noted, that the method used to generate the values in **Table 3**, are subject to systematic user errors. The relative positions of the cross section and the selected area are hand selected but are as close as possible. These are determined using both the Ra and Rq values associated with the selected cross sections. The data is relative to a selected form, in Experiment 1 this is a circle fit, while in Experiment 2 it is a 3rd order polynomial fit. The results shows the expected Ra for the undamaged regular surface is of the order of 1-2 μm , while the corresponding roughness for the structures surfaces is of the order 40-55 μm . It is noted that the Ra values is an arithmetic mean and that the hidden

surfaces (with lower amplitude) will contribute to the lower Ra when compared to the Ra from the optical system, where there is no hidden data all. The similar values for, the overall height Rz (after form fitting), and the distance between the top 4 peaks suggest that the accuracy of the X-CT system is well matched with the calibrated XYRIS 2020 system. The latter system is calibrated system, using standard artefacts. This result although not fully tested, is encouraging for a further investigation of the robustness of the X-CT data.

To enable the application of the Sap parameter on both X-CT and optical surface data, we need to define the reference projected area. In this data a 1mm radius is used. The areas are selected by eye, and because of the nature of the surface this implies a possible systematic error. The results in **table 3**, show that for the selected areas the optical data has a slightly higher surface area. This is probably the consequence of the higher data resolution, since the higher data resolution on a rough surface will by it nature generate a higher surface area. To remove outliers associated with the optical data, a Median filter (3 x 3) has been applied, while no filter has been applied to the X-CT surface data.

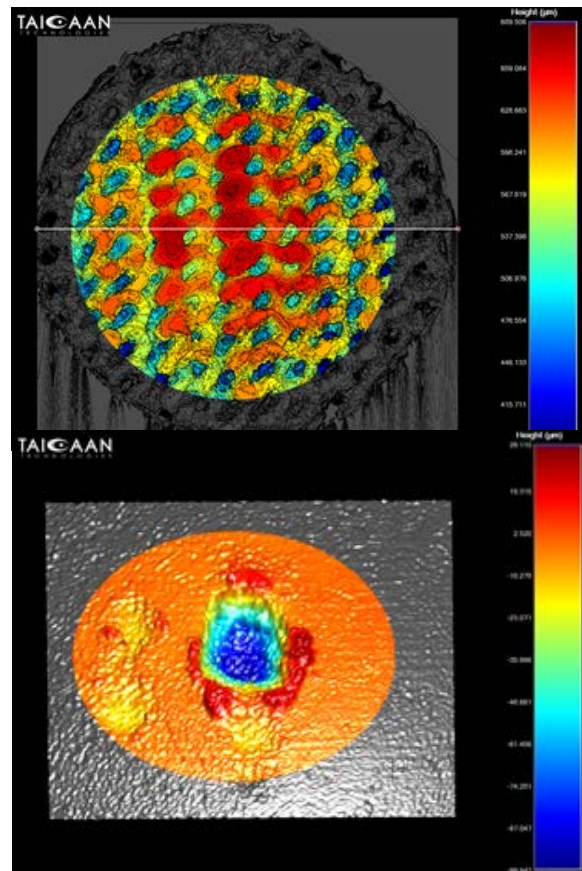


Fig 10. XYRIS data with selected 1 mm radius used for S (a/p) parameter, (upper), while the lower surface is the anode modified using the 3 stage process, and showing the area selected for the volume in Table 2. The anode wear region in **Figure 10**, has been process following the same 3-stage process in experiment 1,

and the resulting volume shown in **Table 2**. This shows a reduction in the wear volume when compared to the data in experiment 1.

4. Conclusions

There are a number of new developments presented in this paper.

1. A new data rendering method is shown which allows surface 3D data to be superimposed on microscope images to provide additional data particularly on a surface where there is no clear change in volume but a darkening of the surface is apparent.
2. The results show that the complexity of the volume fitting methods and the requirement of the application of data registration methods. The current established 3-step method is prone to user error. It has been shown that a small change of 1 μm in the position of the flat surface datum can result in a 15% change in the measured volumes.
3. A new texture parameter is introduced and used in the analysis of a structured cathode surface. The parameter has been used in the evaluation of the structured surface.
4. The paper introduces the application of electron beam forming to create the structured surface.
5. Finally X-CT is used and compared with the established optical methods in the evaluation of the structured surface. It is shown that the X-Ray method is able to show surfaces not visible with conventional optical methods (recesses), and the data processing methods used allow the recessed surfaces to be included in the characterisation of the surface.

Acknowledgements.

The authors would like to thank Ang Zong-Zi (William) for his input in undertaking the X-CT study used in this work; and to Jerry Witter and Zanka Chen of Electrical Contacts Plus (USA) for the supply of the contact materials and housing the switching experiments.

References

- [1] J. Swingler ; J.W. McBride, "The erosion and arc characteristics of Ag/CdO and Ag/SnO₂ contact materials under DC break conditions", IEEE Trans. CPMT, Vol 19, Issue 3, Sept 1996, pp404-415.
- [2]. McBride J.W, Maul C, "The 3D measurement and analysis of high precision surfaces using confocal optical methods", IEICE transactions on electronics, Volume 87, Issue 8, (2004) pp 1261-1267.
- [3]. McBride J.W, "The Volumetric Erosion of Electrical Contacts", IEEE Transactions on Components and Packaging Technology, Vol 23, No 2, June 2000, pp 211-221.
- [4] McBride, J.W. "A review of surface erosion measurements in low voltage switching devices". In, Proceedings of Twenty First International Conference on Electrical Contacts, Zurich, Switzerland, Sep 2002, pp 462-470.
- [5] McBride, J.W. "A review of volumetric erosion studies in low voltage electrical contacts". IEICE Transactions on Electronics, E86-C, (6), 2003, pp 908-914.
- [6] McBride, J.W., Sumption, A.P. and Swingler, J. (2004) On the Evaluation of Low Level Contact Erosion. In, Electrical Contacts, 2004. Proceedings of the 50th IEEE Holm Conference on Electrical Contacts and the 22nd International Conference on Electrical Contacts, 20-23 Sep 2004, pp, 370-377.
- [7] Zhang, D., McBride, J.W. and Hill, M. (2004) A feature extraction method for the assessment of the form parameters of surfaces with localised erosion. Wear, 256, (3-4), 243-251.
- [8] Hasegawa M, Izumi K, Kamada Y, "New algorithm for volumetric analysis of contact damages with laser microscope data", International Conference on Electrical Contacts, 2006, pp 337-342.
- [9] McBride J.W, Chapter 13, "Low Current Switching", 2nd Edition "Electrical contacts (Principles and applications), Ed. Slade. P.G, 2014, pp 731-784.
- [10] D A. Dance, Buxton BG, An introduction to surf-sculpt technology - new opportunities, new challenges, Proceedings of the 7th International Conference on Beam Technology (2007), pp. 75-84
- [11] McBride J.W, Cross K.J, Bull T.G, "Optical metrology for the morphological characterization of surfaces: limitations, innovations, registration, and new directions", Optical Metrology and Inspection for Industrial Applications VI 11189, 111890S, SPIE China, 2019.
- [12] JJ Lifton, A. A. Malcolm, J. W. McBride, (2015), "On the uncertainty of surface determination in X-ray computed tomography for dimensional metrology", Measurement Science and Technology. 26 (3), 2015, 03500.
- [13] JJ Lifton, AA Malcolm, JW McBride, "An experimental study on the influence of scatter and beam hardening in x-ray CT for dimensional metrology", Measurement Science and Technology 27 (1), 2015, 015007.
- [14] BEX®, surface analysis software, from TaiCaan Technologies Ltd. www.taicaan.com